Eur. Phys. J. C (2014) 74:3010
DOI 10.1140/epjc/s10052-014-3010-4

THE EUROPEAN PHYSICAL JOURNAL C

Regular Article - Theoretical Physics

Rare decay $\pi^0 \to e^+e^-$: on corrections beyond the leading order

Tomáš Husek[a], **Karol Kampf**[b], **Jiří Novotný**[c]

Faculty of Mathematics and Physics, Institute of Particle and Nuclear Physics, Charles University, V Holešovičkách 2, Praha 8, Czech Republic

Received: 29 May 2014 / Accepted: 25 July 2014 / Published online: 20 August 2014

Abstract The preceding experimental and theoretical results on the rare decay $\pi^0 \to e^+e^-$ are briefly summarized. Already computed two-loop QED corrections are reviewed and the bremsstrahlung contribution beyond the soft-photon approximation is analytically calculated. The possible further contribution of QCD loop corrections is estimated using the leading logarithm approximation. The complete result can be used to fit the value of the contact interaction coupling $\chi^{(r)}$ to the recent KTeV experiment with the result $\chi^{(r)}(M_\rho) = 4.5 \pm 1.0$.

1 Motivation

Experimental measurements of the rare decay of a neutral pseudoscalar meson to a lepton pair and comparison with theoretical predictions offer an interesting way to study low-energy (long-distance) dynamics in the Standard Model (SM) [1–3]. Systematical theoretical treatment of the process dates back to 1959, when the first prediction of the decay rate was published by Drell [4]. While the possible contributions of the weak sector of the SM are small enough to be neglected, the leading order QED contribution is described by two virtual photon exchange triangle diagram. That is why the double off-shell pion transition form factor $F_{\pi^0\gamma^*\gamma^*}$, which is not known from the first principles, plays an essential role.

Because of this one-loop structure for the leading order, the process is very rare and suppressed in the comparison to two-photon decay ($\pi^0 \to \gamma\gamma$) by a factor of $2(\alpha m_e/M_{\pi^0})^2$ due to the approximate helicity conservation of the interaction and thus may be sensitive to possible effects of the physics beyond the SM (the expected branching ratio from the pure SM calculation is about 10^{-7}).

Recently, this decay has attracted the attention of theorists again in connection with a new precise branching ratio measurement. The KTeV-E799-II experiment at Fermilab [5] has observed $\pi^0 \to e^+e^-$ events (altogether 794 candidates), where $K_L \to 3\pi^0$ decay was used as a source of neutral pions. The KTeV result is

$$\frac{\Gamma(\pi^0 \to e^+e^-,\ x > 0.95)}{\Gamma(\pi^0 \to e^+e^-\gamma,\ x > 0.232)} = (1.685 \pm 0.064 \pm 0.027) \times 10^{-4}. \tag{1}$$

Here we have introduced the Dalitz variable

$$x \equiv \frac{(p+q)^2}{M^2} = \frac{(P-k)^2}{M^2} = 1 - \frac{2E_k}{M}, \tag{2}$$

where p, q, and k are four-momenta of electron, positron, and photon, respectively, $P = (p+q+k)$ is the four-momentum of neutral pion π^0 with a mass M and E_k is the energy of the real outgoing photon in the pion CMS. The lower bound of the Dalitz variable x is used to suppress the contribution of the Dalitz decay $\pi^0 \to e^+e^-\gamma$, which naturally arises with lower x.

By means of extrapolating the Dalitz branching ratio in (1) to the full range of x, the branching ratio of the neutral pion decay into an electron–positron pair was determined to be equal to

$$B(\pi^0 \to e^+e^-(\gamma),\ x > 0.95) = (6.44 \pm 0.25 \pm 0.22) \times 10^{-8}. \tag{3}$$

Here the first error is from data statistics alone and the second is the total systematic error. For the matter of interest, current PDG average value $(6.46 \pm 0.33) \times 10^{-8}$ [6] is mainly based on this new result.

The KTeV Collaboration used the result (3) for further calculations. They used the early calculation of Bergström [7] to extrapolate the full radiative tail beyond $x > 0.95$ and to scale the result back up by the overall radiative corrections of

[a] e-mail: husek@ipnp.mff.cuni.cz
[b] e-mail: karol.kampf@mff.cuni.cz
[c] e-mail: jiri.novotny@mff.cuni.cz

3.4 % to get the lowest order rate (with the final state radiation removed) for $\pi^0 \to e^+e^-$ process. The final result is

$$B^{\text{no-rad}}_{\text{KTeV}}(\pi^0 \to e^+e^-) = (7.48 \pm 0.29 \pm 0.25) \times 10^{-8}. \tag{4}$$

Subsequent comparison with theoretical predictions of the SM was made in [1,2] using pion transition form-factor data from CELLO [8] and CLEO [9] experiments. Finally, it has been found that according to the SM the result should be

$$B^{\text{no-rad}}_{\text{SM}}(\pi^0 \to e^+e^-) = (6.23 \pm 0.09) \times 10^{-8}. \tag{5}$$

This can be interpreted as a 3.3σ discrepancy between the theory and the experiment. Of course, the discrepancy initiated further theoretical investigation of its possible sources [10,11]. Aside from the attempts to find the corresponding mechanism within the physics beyond the SM, also the possible revision of the SM predictions has been taken into account. Many corrections of this kind have been already made, but so far with no such a significant influence on the final result.

2 Leading order

According to the Lorentz symmetry the on-shell invariant matrix element of the $\pi^0 \to e^+e^-$ process can be generally written in terms of just one pseudoscalar form factor

$$i\mathcal{M}(\pi^0 \to e^+e^-) = \overline{u}(p,m)\gamma^5 v(q,m) P(p^2, q^2, P^2) \tag{6}$$

and, as a consequence, the total decay rate is given by

$$\Gamma(\pi^0 \to e^+e^-) = \frac{M}{8\pi}\sqrt{1-v^2}\left|P(m^2, m^2, M^2)\right|^2, \tag{7}$$

where m stands for electron mass and $v \equiv 2m/M$. The leading order in the QED expansion is depicted as the left hand side of the graphical equation in Fig. 1. Here the shaded blob corresponds to the off-shell pion transition form factor $F_{\pi^0\gamma^*\gamma^*}(l^2, (P-l)^2)$ where l is the loop momentum. This form factor serves as an effective UV cut-off due to its $1/l^2$ asymptotics governed by OPE (see e.g. [12]) and the loop integral over $\mathrm{d}^4 l$ is therefore convergent. It is convenient to pick up explicitly the non-analytic contribution of the two-photon intermediate state (the imaginary part[1] is determined uniquely up to the normalization given by the on-shell value of $F_{\pi^0\gamma^*\gamma^*}(0,0) \equiv F_{\pi^0\gamma\gamma}$) and express the form factor in the following way (cf. [13]):

[1] Imaginary part of this contribution is given by Cutkosky rules cutting the two virtual photon lines in the Fig. 1.

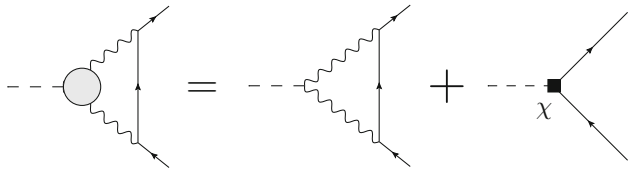

Fig. 1 Leading order contribution in the QED expansion and its representation in terms of the leading order of the chiral perturbation theory

$$\begin{aligned} &P^{\text{LO}}(m^2, m^2, M^2) \\ &\quad = \alpha^2 m F_{\pi^0\gamma\gamma} \frac{1}{\sqrt{1-v^2}} \left[\text{Li}_2(z) - \text{Li}_2\left(\frac{1}{z}\right) + i\pi \log(-z)\right] \\ &\qquad + 2\alpha^2 m F_{\pi^0\gamma\gamma}\left\{\frac{3}{2}\log\left(\frac{m^2}{\mu^2}\right) - \frac{5}{2} + \chi\left(\frac{M^2}{\mu^2}, \frac{m^2}{\mu^2}\right)\right\}. \end{aligned} \tag{8}$$

Here, Li_2 is the dilogarithm,

$$z = -\frac{1-\sqrt{1-v^2}}{1+\sqrt{1-v^2}}, \tag{9}$$

and μ represents the intrinsic scale connected with the form factor[2] $F_{\pi^0\gamma^*\gamma^*}$. The function $\chi(P^2/\mu^2, m^2/\mu^2)$ represents the remainder which collects the contributions of higher intermediate states and is real and analytic[3] for $P^2/\mu^2 < 1$.

The leading order terms in the chiral expansion of the form factor P^{LO} are depicted as the right hand side of the graphical equation in Fig. 1. The $\pi^0\gamma\gamma$ vertex in the loop graph is local and corresponds to the leading order term of the chiral expansion of the form factor $F_{\pi^0\gamma^*\gamma^*}$. Therefore the loop integration is no more UV finite and a counterterm (represented by the tree graph in Fig. 1) is necessary. The sum of these two terms can be written in the form (8), where the transition form factor $F_{\pi^0\gamma\gamma}$ and the remainder $\chi(P^2/\mu^2, m^2/\mu^2)$ are replaced by their leading orders in the chiral expansion,

$$F^{\text{LO}}_{\pi^0\gamma\gamma} = \frac{1}{4\pi^2 F}, \quad \chi^{\text{LO}}(P^2/\mu^2, m^2/\mu^2) = \chi^{(\text{r})}(\mu), \tag{10}$$

where $\chi^{(\text{r})}(\mu)$ is the finite part of the above mentioned counterterm renormalized at scale μ. The graphical equation in Fig. 1 can be understood as the matching condition for $\chi^{(\text{r})}(\mu)$ at the leading order in the chiral expansion. It enables one to determine $\chi^{(\text{r})}(\mu)$ once the form factor $F_{\pi^0\gamma^*\gamma^*}$ is known. The latter can be theoretically modeled e.g. by the

[2] It means the scale at which the loop integral is effectively cut off. The term $\frac{3}{2}\log(m^2/\mu^2)$ represents the leading dependence of the form factor P on this scale.

[3] Note that the higher intermediate states, which appear when also the blob in Fig. 1 is cut, start for $P^2 \sim \mu^2$.

Table 1 Numerical values of $\chi^{(r)}$ in different models according to [1,3]. The first two columns denoted as CLEO+OPE and QCDsr correspond to various treatments of CLEO data. LMD+V is an improvement of the LMD ansatz and NχQM stands for the nonlocal chiral quark model

Model	CLEO+OPE	QCDsr	LMD+V	NχQM
$\chi^{(r)}(M_\rho)$	2.6 ± 0.3	2.8 ± 0.1	2.5	2.4 ± 0.5

lowest meson dominance (LMD) approximation to the large-N_C spectrum of vector-meson resonances, yielding [13]

$$\chi^{(r)}(M_\rho) = 2.2 \pm 0.9, \tag{11}$$

where $M_\rho = 770\,\text{MeV}$ is the mass of the ρ meson. For other alternative estimates cf. Table 1 and for the complete discussion see [1].

Using the value (11) we get for the $\pi^0 \to e^+e^-$ branching ratio numerically

$$B^{\text{LO}}_{\text{SM}}(\pi^0 \to e^+e^-) = (6.1 \pm 0.3) \times 10^{-8}. \tag{12}$$

3 Two-loop virtual radiative corrections

The full two-loop virtual radiative (pure QED) corrections of order $\mathcal{O}(\alpha^3 p^2)$ were calculated in [3]. In this section we will present a short review of the main results.

The relevant contributions to the amplitude are shown in Fig. 2. There are six two-loop diagrams. Listed sequentially, we have two vertex corrections (a, b), electron self-energy insertion (c), box-type correction (d), and two vacuum polarization insertions (e, f). Of course, for every such diagram a one-loop graph with corresponding counterterm must be added to renormalize the subdivergences. The relevant finite parts of these counterterms can be fixed by the requirement that the parameters m and α coincide with their physical values. After the subdivergences are canceled, the remaining superficial divergences has to be renormalized by another additional tree counterterm with coupling ξ. The finite part $\xi^{(r)}(\mu)$ of this coupling has been estimated in [3] using its running with the renormalization scale as

$$\xi^{(r)}(M_\rho) = 0 \pm 5.5. \tag{13}$$

Besides the UV divergences, the graph d in the Fig. 2 is also IR divergent. It is therefore necessary to consider IR-safe decay width of the inclusive process $\pi^0 \to e^+e^-(\gamma)$ with additional real photon in the final state. In [3] the real photon bremsstrahlung has been taken into account using the soft-photon approximation. The final result depends on the experimental upper bound on the soft photon energy which can be expressed in terms of the lower bound x^{cut} on the

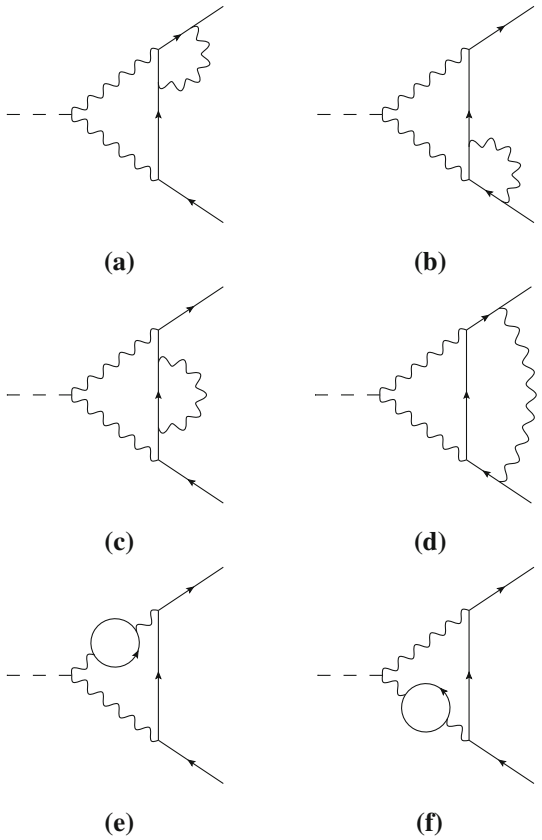

Fig. 2 Two-loop virtual radiative corrections for $\pi^0 \to e^+e^-$ process

Dalitz variable x (see 2). The result can be expressed in terms of the correction factor $\delta(x^{\text{cut}})$ defined as

$$\begin{aligned}&\Gamma^{\text{NLO}}(\pi^0 \to e^+e^-(\gamma),\ x > x^{\text{cut}})\\ &\quad \equiv \delta(x^{\text{cut}})\Gamma^{\text{LO}}(\pi^0 \to e^+e^-),\end{aligned} \tag{14}$$

where Γ^{LO} is the leading order width and Γ^{NLO} is the next-to leading $\mathcal{O}(\alpha^3 p^2)$ correction. The x^{cut} dependent overall correction $\delta(x^{\text{cut}})$ has various sources and to emphasize the origin of its constituents, we will use the same symbol decorated with appropriate indices. For the complete QED two-loop correction $\delta^{(2)}$ including soft-photon bremsstrahlung and KTeV cut $x^{\text{cut}} = 0.95$, in [3] one obtained

$$\delta^{(2)}(0.95) \equiv \delta^{\text{virt.}} + \delta^{\text{BS}}_{\text{soft}}(0.95) = (-5.8 \pm 0.2)\,\%, \tag{15}$$

where only the uncertainties of $\chi^{(r)}$ and $\xi^{(r)}$ were taken as the source of the error. This result differs significantly from the previous approximate calculations done by Bergström [7] or Dorokhov et al. [10], where for $\delta^{(2)}(0.95)$ we would get -13.8 and $-13.3\,\%$, respectively.

There is a simple interrelation of this partial result of the QED radiative corrections and the branching ratio (3) obtained by KTeV experiment (for the details see [3]). We

can write the theoretical prediction for the branching ratio measured by KTeV as

$$B(\pi^0 \to e^+e^-(\gamma),\ x > 0.95) = \frac{\Gamma^{\rm LO}(\pi^0 \to e^+e^-)}{\Gamma(\pi^0 \to \gamma\gamma)} \times B(\pi^0 \to \gamma\gamma)[1 + \delta^{(2)}(0.95) + \Delta^{\rm BS}(0.95) + \delta^{\rm D}(0.95)], \tag{16}$$

where the only experimental input is the precise branching ratio $B(\pi^0 \to \gamma\gamma) = (98.823 \pm 0.034)\,\%$. In the above formula,

$$\delta^{\rm D}(x^{\rm cut}) = \frac{1}{\Gamma^{\rm LO}(\pi^0 \to e^+e^-)} \int_{x^{\rm cut}}^1 {\rm d}x \left(\frac{{\rm d}\Gamma^{\rm Dalitz}}{{\rm d}x}\right)^{\rm NLO}_{1\gamma IR} = \frac{1.75 \times 10^{-15}}{[\Gamma^{\rm LO}(\pi^0 \to e^+e^-)/{\rm MeV}]} \tag{17}$$

corresponds to the unsubtracted fraction of the Dalitz decay background[4] omitted in the KTeV analysis and discussed in [3,14]. In what follows we will concentrate on the last missing ingredient of the formula (16), namely

$$\Delta^{\rm BS}(x^{\rm cut}) \equiv \delta^{\rm BS}(x^{\rm cut}) - \delta^{\rm BS}_{\rm soft}(x^{\rm cut}), \tag{18}$$

which is the difference between the exact bremsstrahlung and its soft photon approximation. This difference has been only roughly estimated in [3] and this estimate has been taken as a source of the error. Our aim is to calculate $\Delta^{\rm BS}$ exactly and test the adequacy of the soft photon approximation for the cut $x^{\rm cut} = 0.95$ used in the KTeV analysis.

4 Bremsstrahlung

In this section, we discuss the above mentioned exact bremsstrahlung (BS), i.e. the real radiative correction corresponding to the process $\pi^0 \to e^+e^-(\gamma)$ beyond the soft-photon approximation. As a consequence of the gauge invariance, the invariant amplitude for the BS correction,

$$\mathcal{M}_{(\lambda)}(p,q,k) \equiv \varepsilon^{*\rho}_{(\lambda)}(k)\mathcal{M}^{\rm BS}_\rho(p,q,k) \tag{19}$$

(where k and $\varepsilon^{*\rho}_{(\lambda)}(k)$ is the photon momentum and polarization vector, respectively), has to satisfy the Ward identity

$$k^\rho \mathcal{M}^{\rm BS}_\rho = 0 \tag{20}$$

for on-shell k and thus it can be generally expressed in the form [14]

$$\begin{aligned} i\mathcal{M}^{\rm BS}_\rho(p,q,k) = {} & \frac{ie^5}{8\pi^2 F} \\ & \times \{P(x,y)[(k\cdot p)q_\rho - (k\cdot q)p_\rho][\bar u(p,m)\gamma_5 v(q,m)] \\ & + A(x,y)[\bar u(p,m)[\gamma_\rho(k\cdot p) - p_\rho(k\cdot\gamma)]\gamma_5 v(q,m)] \\ & - A(x,-y)[\bar u(p,m)[\gamma_\rho(k\cdot q) - q_\rho(k\cdot\gamma)]\gamma_5 v(q,m)] \\ & + T(x,y)[\bar u(p,m)\gamma_\rho \not{k}\gamma_5 v(q,m)]\} \end{aligned} \tag{21}$$

in terms of the scalar form factors P, A, and T. These are functions of two independent kinematic variables (x, y), defined as

$$x = \frac{(p+q)^2}{M^2}, \quad y = -\frac{2}{M^2}\left[\frac{k\cdot(p-q)}{1-x}\right]$$
$$x \in [\nu^2, 1], \quad y \in \left[-\sqrt{1-\frac{\nu^2}{x}}, \sqrt{1-\frac{\nu^2}{x}}\right]. \tag{22}$$

As mentioned above, x is the Dalitz variable (i.e. a normalized square of the total energy of e^+e^- pair in their CMS) and y has the meaning of a rescaled cosine of the angle included by the directions of outgoing photon and positron in the e^+e^- CMS. The modulus squared of the amplitude has the form [14]

$$\begin{aligned} \overline{\left|\mathcal{M}^{\rm BS}(x,y)\right|^2} \equiv {} & \sum_{\rm polarizations} \left|\mathcal{M}_{(\lambda)}(p,q,k)\right|^2 = \\ = {} & \frac{16\pi\alpha^5}{F^2}\frac{M^4(1-x)^2}{8}\Big\{M^2[x(1-y^2)-\nu^2][xM^2|P|^2 \\ & + 2\nu M\,{\rm Re}\{P^*[A(x,y)+A(x,-y)]\} - 4\,{\rm Re}\{P^*T\}] \\ & + 2M^2(x-\nu^2)(1-y)^2|A(x,y)|^2 + (y\to -y) \\ & - 8\nu M y(1-y)\,{\rm Re}\{A(x,y)T^*\} + (y\to -y) \\ & - 4\nu^2M^2y^2\,{\rm Re}\{A(x,y)A(x,-y)^*\} + 8(1-y^2)|T|^2\Big\} \end{aligned} \tag{23}$$

and using the variables x, y the differential decay rate is

$${\rm d}\Gamma^{\rm BS}(x,y) = \frac{M}{(8\pi)^3}\overline{\left|\mathcal{M}^{\rm BS}(x,y)\right|^2}(1-x)\,{\rm d}x\,{\rm d}y. \tag{24}$$

To the amplitude $\mathcal{M}_{(\lambda)}(p,q,k)$ five Feynman diagrams contribute (cf. Fig. 3). Four of them correspond to the photon emission from the outgoing fermion lines (see Fig. 3a–d). Naively, one would expect that only these four diagrams are necessary to consider since only they include IR divergences which are needed to cancel the IR divergences stemming from the virtual corrections (see graph d in Fig. 2 and the corresponding one-loop diagram with counterterm). However, this result would not be complete.

[4] This fraction comes form the contribution of the interference term of the NLO one-photon-irreducible ($1\gamma IR$) graph with the leading order Dalitz amplitude. See [3] and [14] for more details.

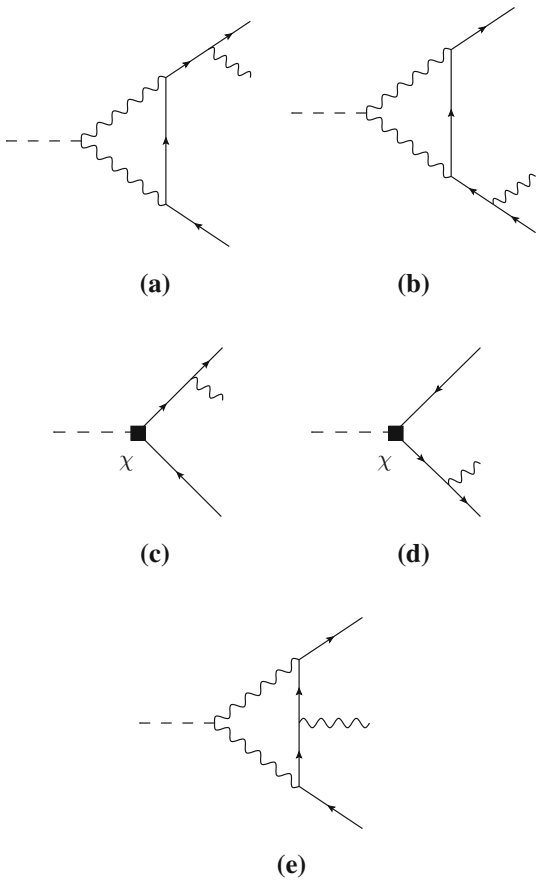

Fig. 3 Bremsstrahlung Feynman diagrams for $\pi^0 \to e^+e^-$ process including counterterms

The reason is that the Ward identity (20) would be violated.[5] Thus it is necessary to add the third (box) diagram (Fig. 3e, photon emitted from the inner fermion line) to fulfill this relation.

In the graphs Fig. 3a and b the $\pi\gamma\gamma$ vertex stems from the Wess–Zumino–Witten action [15,16] and the remaining vertices correspond to standard QED Feynman rules. These graphs are UV divergent by power counting and have to be regularized. In what follows, we use the dimensional regularization. In order to bypass the problems with intrinsically four-dimensional objects like γ_5 and the Levi-Civita pseudo-tensor $\varepsilon^{\mu\nu\alpha\beta}$, we use its variant known as Dimensional Reduction[6] (cf. [17]), which keeps the algebra of γ-matrices four-dimensional, while the loop tensor integrals are regularized dimensionally and expressed in terms of the scalar one-loop integrals using the Passarino–Veltman reduction [18]. Within this framework we first get rid of the Levi-Civita tensor using the four-dimensional identities, e.g.

$$\begin{aligned} \varepsilon^{\alpha\beta\mu\nu}\gamma_\mu\gamma_\nu &= i\gamma_5[\gamma^\alpha, \gamma^\beta] \\ \varepsilon^{\alpha\beta\mu\nu}\gamma_\mu\gamma_\rho\gamma_\nu &= 2i\gamma_5(g^\alpha_\rho\gamma^\beta - g^\beta_\rho\gamma^\alpha), \end{aligned} \tag{25}$$

and then contract the reduced tensor integrals with the γ-matrix structures.[7] The contributions of the box diagram Fig. 3e turn out to be finite, while the triangle diagrams Fig. 3a and b contain subdivergences which have to be renormalized by means of the tree graphs with counterterms corresponding to the coupling χ (see Fig. 3c, d). Summing all the relevant contributions and using the four-dimensional Dirac algebra, we get finally the form factors P, A, and T, the explicit form of which is summarized in Appendix A.

The differential decay rate $\mathrm{d}\Gamma^{\mathrm{BS}}(x, y)$ (cf. 24) give rise to IR divergences when integrated over the phase space. The divergences originate from the soft-photon region

$$|\mathbf{k}| < \frac{1}{2}M(1 - x^{\mathrm{cut}}), \tag{26}$$

which is defined in terms of the variables (x, y) by means of the cut on the Dalitz variable $x > x^{\mathrm{cut}}$. These divergences are exactly the same as those stemming from an analogous integral of the differential decay rate $\mathrm{d}\Gamma^{\mathrm{BS}}_{\mathrm{soft}}(x, y)$ calculated within the soft-photon approximation. The latter is already included in the two-loop result [3], we therefore present our result for the exact BS as the difference

$$\mathrm{d}\Gamma^{\mathrm{BS}}_{\mathrm{diff}}(x, y) = \mathrm{d}\Gamma^{\mathrm{BS}}(x, y) - \mathrm{d}\Gamma^{\mathrm{BS}}_{\mathrm{soft}}(x, y), \tag{27}$$

the integral of which is IR finite. The result for $\mathrm{d}\Gamma^{\mathrm{BS}}_{\mathrm{diff}}(x, y)$ is shown in Fig. 4 and (integrated over the allowed region of y given by 22) in Fig. 5. For $\Delta^{\mathrm{BS}}(x^{\mathrm{cut}})$ we get finally

$$\Delta^{\mathrm{BS}}(x^{\mathrm{cut}}) = 2\int_{x^{\mathrm{cut}}}^{1}\int_{0}^{\sqrt{1-\nu^2/x}} \frac{\mathrm{d}\Gamma^{\mathrm{BS}}_{\mathrm{diff}}(x, y)}{\Gamma^{\mathrm{LO}}(\pi^0 \to e^+e^-)}. \tag{28}$$

The dependence of $\Delta^{\mathrm{BS}}(x^{\mathrm{cut}})$ on x^{cut} is shown in Fig. 6. For $x^{\mathrm{cut}} = 0.95$ and for $\chi^{(\mathrm{r})}$ given by (11) we get numerically

$$\Delta^{\mathrm{BS}}(0.95) = (0.30 \pm 0.01)\,\%, \tag{29}$$

where the error stems from the uncertainty in $\chi^{(\mathrm{r})}(M_\rho)$. In other words, using this cut of the Dalitz variable in the KTeV experiment, the soft-photon approximation is a very good approach to the exact result. The dependence of $\Delta^{\mathrm{BS}}(0.95)$ on $\chi^{(\mathrm{r})}$ is shown in Fig. 7.

[5] Note that in the framework of the soft-photon approximation the sum of these four graphs satisfies the Ward identity by itself.

[6] Note, however, that in the general case the regularization by dimensional reduction might spoil gauge invariance. In the case of our amplitude, we have checked that the gauge invariance is preserved and the regularized amplitude has the general form (21).

[7] According to the prescription [17], we take the metric tensors stemming from the Passarino–Veltman reduction effectively as four-dimensional.

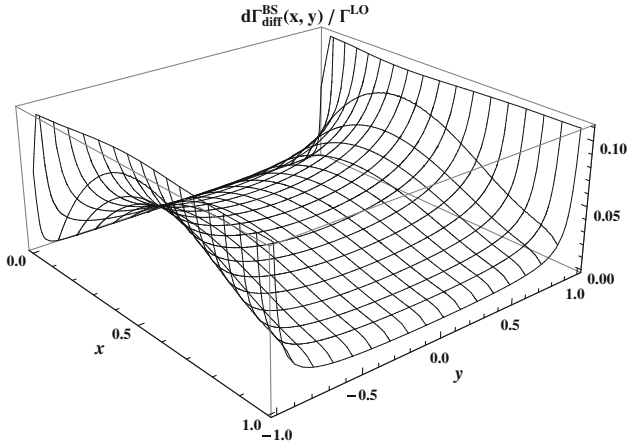

Fig. 4 3D plot of $\mathrm{d}\Gamma^{\mathrm{BS}}_{\mathrm{diff}}(x, y)$ normalized to the leading order contribution of the $\pi^0 \to e^+e^-$ process

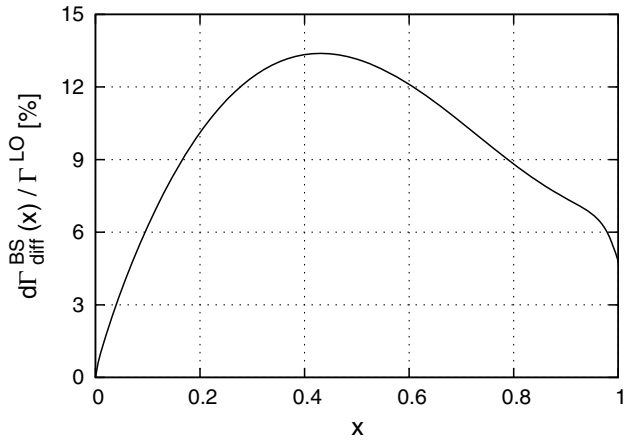

Fig. 5 Plot of $\mathrm{d}\Gamma^{\mathrm{BS}}_{\mathrm{diff}}(x) = \int \mathrm{d}\Gamma^{\mathrm{BS}}_{\mathrm{diff}}(x, y)\,\mathrm{d}y$ normalized to the leading order contribution of the $\pi^0 \to e^+e^-$ process

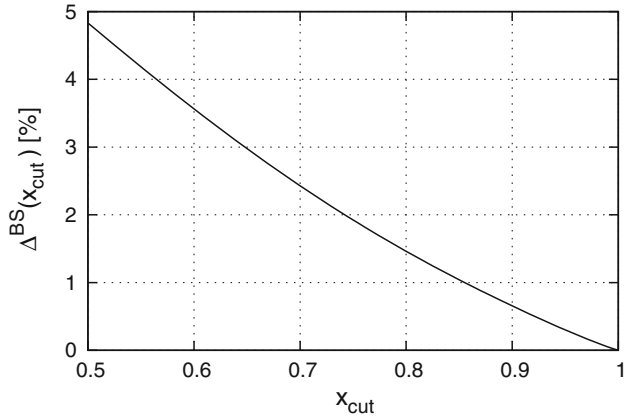

Fig. 6 The dependence of Δ^{BS} on the cut on the Dalitz variable

Now we have all ingredients needed in Eq. (16) under control and we can thus fit the value of the coupling $\chi^{(\mathrm{r})}$ to meet the experiment with the result

$$\chi^{(\mathrm{r})}(M_\rho) = 4.5 \pm 1.0. \tag{30}$$

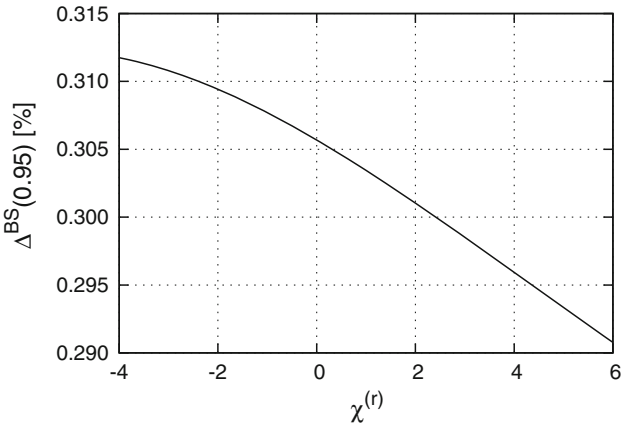

Fig. 7 The dependence of $\Delta^{\mathrm{BS}}(0.95)$ on $\chi^{(\mathrm{r})}$. It is apparent that the dependence is very slight and can be neglected in the calculation of the $\chi^{(\mathrm{r})}$

The error is dominated by the experimental uncertainty, while the theoretical error corresponding to the estimate (13) is negligible. To compare, some previously estimated values, which were considered as relevant, are shown in Table 1.

5 Estimate of the theoretical uncertainty of $\chi^{(\mathrm{r})}$

The above determination of $\chi^{(\mathrm{r})}$ represents an effective LO value of this coupling and includes therefore implicitly higher order chiral contributions. The corrections to the LO value of $\chi^{(\mathrm{r})}$ start at the NLO and stem from the two-loop graphs which correspond to a substitution of the one-loop subgraphs (and corresponding counterterms) for the shaded blob on the left hand side of the graphical equation depicted in Fig. 1. The relative size of such corrections is set by the factor $(M/4\pi F)^2 \sim 10^{-2}$ and can be naively treated as negligible, however, it can be significantly numerically enhanced by the large double logarithm terms like $\log^2(\mu^2/m^2) \sim 10^2$ for $\mu \sim M_\rho$.

A complete calculation of the NLO corrections is beyond the scope of the present article. In this section, we will only restrict ourselves to the rough estimate based on explicit calculation of the above mentioned leading (double) logarithms, which are expected to represent a numerically relevant part of the full NLO contribution. According to the Weinberg consistency relation [19], this can be achieved by means of an evaluation of infinite parts of one-loop graphs only. In what follows, we will adapt this relation to our case.

Let us write the contribution of the above mentioned two-loop graphs as

$$P^{\mathrm{NLO}} = P^{\text{2-loop}} + P^{\text{1-loop}}_{\mathrm{CT}} + P^{\mathrm{tree}}_{\mathrm{CT}} + (Z^{\text{1-loop}})^{\frac{1}{2}} P^{\mathrm{LO}}, \tag{31}$$

where the first three terms correspond to one-particle irreducible (1PI) contributions (including two-loop graphs, one-

loop graphs with counterterms and tree counterterm graphs) and the last term represents the renormalization of the external pion line by means of the one-loop Z-factor. The contributions of the 1PI loop graphs $P^{\text{2-loop}}$ can be written schematically[8] as an expansion in $\varepsilon = 2 - \frac{d}{2}$

$$P^{\text{2-loop}} = \mu^{-4\varepsilon}\left(\frac{\mu^2}{m^2}\right)^{2\varepsilon} \times\left[\frac{P^{\text{2-loop}}_{-2}}{\varepsilon^2} + \frac{P^{\text{2-loop}}_{-1}}{\varepsilon} + \mathcal{O}(\varepsilon^0)\right]. \tag{32}$$

In the same way, for $P^{\text{1-loop}}_{\text{CT}}$ we get (see Fig. 8)

$$P^{\text{1-loop}}_{\text{CT}} = \mu^{-4\varepsilon}\left(\frac{\mu^2}{m^2}\right)^{\varepsilon} \times\Bigg[\sum_{i=7,11,13}\left(c_i^{W(\text{r})}(\mu) - \frac{\eta_i^W}{32\pi^2\varepsilon}\right)\left(\frac{P^{\text{1-loop}}_{i,-1}}{\varepsilon} + \mathcal{O}(\varepsilon^0)\right) + \left(\chi^{(\text{r})}(\mu) - \frac{\eta_\chi}{32\pi^2\varepsilon}\right)\left(\frac{P^{\text{1-loop}}_{\chi,-1}}{\varepsilon} + \mathcal{O}(\varepsilon^0)\right)\Bigg] \tag{33}$$

and the one-loop ingredients of the term $(Z^{\text{1-loop}})^{1/2}P^{\text{LO}}$ are then in the same way (see Fig. 9)

$$\begin{aligned}(Z^{\text{1-loop}})^{\frac{1}{2}} &= \mu^{-2\varepsilon}\Bigg[\left(\frac{\mu^2}{m^2}\right)^{\varepsilon}\left(\frac{Z^{\frac{1}{2},\text{1-loop}}_{-1}}{\varepsilon} + \mathcal{O}(\varepsilon^0)\right) + \beta_4\left(l_4^{(\text{r})}(\mu) - \frac{\gamma_4}{32\pi^2\varepsilon}\right)\Bigg]\\ P^{\text{LO}} &= \mu^{-2\varepsilon}\Bigg[\left(\frac{\mu^2}{m^2}\right)^{\varepsilon}\left(\frac{P^{\text{LO}}_{-1}}{\varepsilon} + \mathcal{O}(\varepsilon^0)\right) + \beta_\chi\left(\chi^{(\text{r})}(\mu) - \frac{\eta_\chi}{32\pi^2\varepsilon}\right)\Bigg].\end{aligned} \tag{34}$$

Here $l_i^{(\text{r})}(\mu)$, $c_i^{W(\text{r})}(\mu)$, and $\chi^{(\text{r})}(\mu)$ are finite parts of the one-loop counterterms. We use the standard notation for the two-flavor Chiral Perturbation theory (ChPT) both in the even [20,21] and in the odd sector [22]. The coefficient β_χ can be obtained from (8) and (10):

$$\beta_\chi = \frac{1}{2}\left(\frac{\alpha}{\pi}\right)^2\frac{m}{F} \tag{35}$$

and β_4 will be discussed below. The Weinberg condition is based on absence of nonlocal divergences of the form $\log(\mu^2)/\varepsilon$. It can be expressed as the following constraint:

[8] Because we are interested only in the singular parts we ignore the difference between MS, $\overline{MS}$, and $\overline{MS}_\chi$ subtraction schemes in what follows. Such an omission can affect only the finite parts which are irrelevant for the leading log calculation.

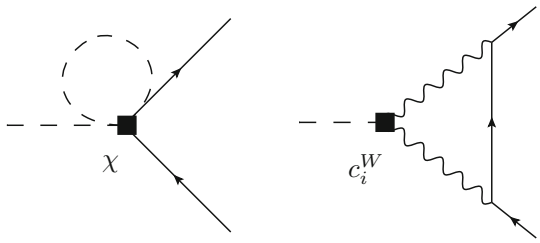

Fig. 8 One-loop diagrams of order α^2/F^3 for $\pi^0 \to e^+e^-$ process

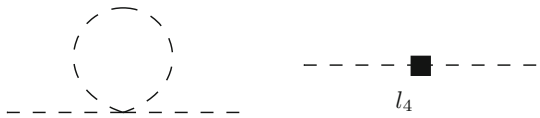

Fig. 9 Z-factor contributions

$$0 = 2P^{\text{2-loop}}_{-2} - \sum_{i=7,11,13}\left(\frac{\eta_i^W P^{\text{1-loop}}_{i,-1}}{32\pi^2}\right) - \frac{\eta_\chi P^{\text{1-loop}}_{\chi,-1}}{32\pi^2} + 2Z^{\frac{1}{2},\text{1-loop}}_{-1}P^{\text{LO}}_{-1} - Z^{\frac{1}{2},\text{1-loop}}_{-1}\frac{\beta_\chi\eta_\chi}{32\pi^2} - \frac{\beta_4\gamma_4 P^{\text{LO}}_{-1}}{32\pi^2}. \tag{36}$$

The contribution of the leading double logs P^{LL} is

$$P^{\text{LL}} = \frac{1}{2}\log^2\left(\frac{\mu^2}{m^2}\right) \times\Bigg[4P^{\text{2-loop}}_{-2} - \sum_{i=7,11,13}\left(\frac{\eta_i^W P^{\text{1-loop}}_{i,-1}}{32\pi^2}\right) - \frac{\eta_\chi P^{\text{1-loop}}_{\chi,-1}}{32\pi^2} + 4Z^{\frac{1}{2},\text{1-loop}}_{-1}P^{\text{LO}}_{-1} - Z^{\frac{1}{2},\text{1-loop}}_{-1}\frac{\beta_\chi\eta_\chi}{32\pi^2} - \frac{\beta_4\gamma_4}{32\pi^2}\Bigg]. \tag{37}$$

Using the constraint (36), we get finally

$$P^{\text{LL}} = \left(\frac{1}{8\pi}\right)^2\log^2\left(\frac{\mu^2}{m^2}\right)\Bigg[\sum_{i=7,11,13}\left(\eta_i^W P^{\text{1-loop}}_{i,-1}\right) + \eta_\chi P^{\text{1-loop}}_{\chi,-1} + \beta_\chi\eta_\chi Z^{\frac{1}{2},\text{1-loop}}_{-1} + \beta_4\gamma_4 P^{\text{LO}}_{-1}\Bigg]. \tag{38}$$

Let us now discuss the ingredients of the formula (38). The infinite parts of the couplings χ and l_4 are

$$\gamma_4 = 2\,, \quad \frac{\eta_\chi}{32\pi^2} = -\frac{3}{2}. \tag{39}$$

From the finiteness of P^{LO}, it follows that

$$P^{\text{LO}}_{-1} = \frac{\beta_\chi\eta_\chi}{32\pi^2} = -\frac{3}{4}\left(\frac{\alpha}{\pi}\right)^2\frac{m}{F}. \tag{40}$$

For the couplings c_i^W, the infinite parts depend on the form of the l_4 term in the chiral Lagrangian (see [23–25] for details). For the standard choice

$$\mathcal{L}_4^{\text{std}} = \frac{il_4}{4}\langle u^\mu \chi_{\mu-}\rangle \tag{41}$$

we get

$$\eta_7^W = \eta_{11}^W = -\eta_{13}^W = \frac{1}{32\pi^2 F^2} \tag{42}$$

(in this case, $\beta_4 = 0$), while for the equivalent case, which differs by terms proportional to the LO equation of motion,

$$\begin{aligned}\mathcal{L}_4 &= \frac{l_4}{8}\langle u^\mu u_\mu\rangle\langle\chi_+\rangle \\ &= \frac{il_4}{4}\langle u^\mu \chi_{\mu-}\rangle + \frac{il_4}{4}\left\langle \widehat{\chi}_-\left(\nabla_\mu u^\mu - \frac{i}{2}\widehat{\chi}_-\right)\right\rangle,\end{aligned} \tag{43}$$

we get $\beta_4 = -(M/F)^2$ and

$$4\eta_7^W = \eta_{11}^W = -\eta_{13}^W = \frac{1}{32\pi^2 F^2}. \tag{44}$$

Because both choices have to lead to the same result, we get the following relation:

$$\frac{P_{7,-1}^{\text{1-loop}}}{(8\pi F)^2} = -\frac{2}{3}\beta_4\gamma_4 P_{-1}^{\text{LO}} = \left(\frac{\alpha}{\pi}\right)^2 \frac{m}{F}\left(\frac{M}{F}\right)^2. \tag{45}$$

The Z-factor is not a physical observable; therefore it is both sensitive to the field redefinition and in principle infinite. To calculate it we will use the exponential parametrization $U = \exp(i\phi/F)$ (see e.g. [24]):

$$Z_{-1}^{\frac{1}{2},\text{1-loop}} = -\frac{1}{3}\left(\frac{M}{4\pi F}\right)^2. \tag{46}$$

The only missing ingredients are then $P_{11,-1}^{\text{1-loop}}$, $P_{13,-1}^{\text{1-loop}}$, and $P_{\chi,-1}^{\text{1-loop}}$, which correspond to the one-loop graphs depicted in the Fig. 8. Explicitly, we get

$$P_{\chi,-1}^{\text{1-loop}} = \frac{2}{3}\left(\frac{\alpha}{\pi}\right)^2 \frac{m}{F}\left(\frac{M}{4\pi F}\right)^2, \tag{47}$$

$$P_{11,-1}^{\text{1-loop}} = -\frac{1}{4}P_{7,-1}^{\text{1-loop}}, \tag{48}$$

$$P_{13,-1}^{\text{1-loop}} = -\left(\frac{4\pi}{3}\right)^2\left(\frac{\alpha}{\pi}\right)^2 \frac{m}{F}M^2\left(1-\frac{5}{2}\nu^2\right). \tag{49}$$

Putting all these ingredients together, we find that

$$\begin{aligned}&\sum_{i=7,11}\eta_i^W P_{i,-1}^{\text{1-loop}} + \eta_\chi P_{\chi,-1}^{\text{1-loop}} + \beta_\chi\eta_\chi Z_{-1}^{\frac{1}{2},\text{1-loop}} \\ &\quad + \beta_4\gamma_4 P_{-1}^{\text{LO}} = 0,\end{aligned} \tag{50}$$

and we get finally

$$\begin{aligned}P^{\text{LL}} &= \left(\frac{1}{8\pi}\right)^2 \eta_{13}^W P_{13,-1}^{\text{1-loop}} \log^2\left(\frac{\mu^2}{m^2}\right) \\ &= \frac{1}{72}\left(\frac{\alpha}{\pi}\right)^2 \frac{m}{F}\left(\frac{M}{4\pi F}\right)^2\left(1-\frac{5}{2}\nu^2\right)\log^2\left(\frac{\mu^2}{m^2}\right),\end{aligned} \tag{51}$$

which implies the following leading log correction, which has to be subtracted from the experimentally determined coupling (30):

$$\begin{aligned}\Delta^{\text{LL}}\chi^{(\text{r})}(\mu) &= \beta_\chi^{-1} P^{\text{LL}} \\ &= \frac{1}{36}\left(\frac{M}{4\pi F}\right)^2\left(1-\frac{5}{2}\nu^2\right)\log^2\left(\frac{\mu^2}{m^2}\right).\end{aligned} \tag{52}$$

Numerically

$$\Delta^{\text{LL}}\chi^{(\text{r})}(M_\rho) = 0.081, \tag{53}$$

which is well below the uncertainty of $\chi^{(\text{r})}$ in (30). This can be taken as an indication of the robustness of our determination of $\chi^{(\text{r})}$ with respect to the NLO chiral corrections.

6 Conclusion

In this article we have revisited the decay $\pi^0 \to e^+e^-$. It has attracted a lot of attention since its recent precise measurement by KTeV Collaboration at Fermilab due to the discrepancy with the theoretical predictions. Provided that the measured quantity is in agreement with the future experiments one can attribute the existing discrepancy to the quantum corrections, correct modeling of the double off-shell pion transition form factor $F_{\pi^0\gamma^*\gamma^*}$, and/or possible contribution of new physics. Our focus here was on the first part, i.e. SM corrections to the leading order calculation. We have first briefly summarized recent precise theoretical works dealing with the two-loop QED corrections. The missing bremsstrahlung contribution to this process has been calculated. We have shown that the soft-photon approximation is an adequate approach in the region of KTeV experiment. Besides the electromagnetic corrections we have also studied possible stability in the strong sector. It is best modeled using the higher pion-loop contributions, for example in the framework of $SU(2)$ ChPT. It is often the case that in the two-flavor ChPT the order of these corrections can be estimated by the size of the chiral logarithms. In fact they represent the potential enhancement of the usual counting. We have explicitly calculated the coefficient of the leading logarithm and due to the large suppression factor 1/72 (see 51) it turns out to be very small. This might be an indication of the fast convergence of the

perturbation series which is a situation similar to the chiral corrections of $\pi^0 \to \gamma^{(*)}\gamma^{(*)}$ decay (cf. [25,26]).

Using the most reliable QCD modeling of the $F_{\pi^0\gamma^*\gamma^*}$ via the lowest-meson dominance approach [13] we agree with the estimate made in [3] of 2σ discrepancy between the theory (including all radiative corrections) and the experiment. Let us recall that this number is significantly smaller than the difference usually quoted (3.3σ); however, let us stress that this bigger number was obtained from the rough estimates of the QED radiative corrections and it is thus an indication of the importance of the full two-loop calculation for this process.

On the other hand, the still unsatisfactory situation in the first-principle modeling of the three-point vector–vector–pseudoscalar correlator leads to the possibility to use the precise measurement and the full radiative calculation of this process to set the hadronic form factor, represented for this process by the constant χ. The obtained value $\chi^{(\mathrm{r})}(M_\rho) = 4.5 \pm 1.0$ (see 30) is slightly different from the usual estimations; however, it represents the model independent prediction for this quantity, based on the KTeV experiment. It can be further used e.g. in the hadronic light-by-light contribution of the muon $g-2$ (see e.g. [27,28] for details).

Acknowledgments This work is supported by Charles University in Prague, project PRVOUK P45, and by Ministry of Education of the Czech Republic, grant LG 13031. T.H. was supported by the grants SVV 260097/2014 and GAUK 700214.

Appendix A: Explicit form of the bremsstrahlung form factors

In Sect. 4 we have defined the invariant amplitude for the bremsstrahlung correction $\mathcal{M}_\rho^{\mathrm{BS}}$ using the form factors P, A, and T. In this appendix we will summarize their explicit form using the standard Passarino–Veltman scalar one-loop integrals B_0, C_0, and D_0. The only divergent function is then B_0. Its explicit form will be given here as a reference point for our notation:

$$i\pi^2 B_0(0,m^2,m^2) = (2\pi)^4\mu^{4-d}\int \frac{\mathrm{d}^d l}{(2\pi)^d}\frac{1}{[l^2-m^2+i\epsilon]^2} = i\pi^2\left[\frac{1}{\varepsilon}-\gamma_E+\log 4\pi+\log\left(\frac{\mu^2}{m^2}\right)\right], \tag{54}$$

where we have introduced $\varepsilon = 2-\frac{d}{2}$. Note that in this regularization scheme the bare counterterm coupling χ is given by [13,29]

$$\chi = \frac{3}{2}\left(\frac{1}{\varepsilon}-\gamma_E+\log 4\pi\right)+\chi^{(\mathrm{r})}(\mu). \tag{55}$$

The bremsstrahlung form factors are

$$\begin{aligned}
-16i\pi^2 P(x,y) &= \frac{2\nu}{M(1-x)^2(1-y^2)}\\
&\times\left\{-\frac{4}{M^2}[3B_0(0,m^2,m^2)-2\chi+5]+\frac{1}{[x(1-y^2)-\nu^2]}\right.\\
&\times[2x(1-x)(1-y^2)(1-y)C_0(m^2,0,K_-^2,0,m^2,m^2)\\
&+2(1+y)[x(1-y^2)+x^2(1-y)^2-2\nu^2]\\
&\times C_0(m^2,M^2,K_-^2,m^2,0,0)\\
&+\frac{M^2}{2}(1-x)(1-y^2)[x(1-x)(1-y^2)-2\nu^2]\\
&\left.\times D_0(m^2,M^2,m^2,0,K_-^2,K_+^2,m^2,0,0,m^2)\right]\\
&+(y\to -y),
\end{aligned} \tag{56}$$

$$\begin{aligned}
-16i\pi^2 A(x,y) &= -\frac{8}{M^2[2(1-x)(1-y)+\nu^2]}\\
&-\frac{4\nu^2}{M^2(1-x)^2(1-y)^2}\times\left\{-2+\frac{3(1-x)(1-y)+\nu^2}{2(1-x)(1-y)+\nu^2}\right.\\
&\left.\times[B_0(K_-^2,0,m^2)-B_0(0,m^2,m^2)]\right\}\\
&-\frac{2\nu^2}{(1-x)(1-y)}C_0(m^2,0,K_-^2,0,m^2,m^2)\\
&-\frac{1}{2[x(1-y^2)-\nu^2]}\\
&\times\left\{-2(1-y)[(1-x)(1-y^2)+2\nu^2]\right.\\
&\times C_0(m^2,0,K_-^2,0,m^2,m^2)+(y\to -y)\\
&+\left[2(1-y^2)[1+x+(1-x)y]+\frac{8\nu^2 y}{1-x}\right]\\
&\times C_0(m^2,M^2,K_-^2,m^2,0,0)+(y\to -y)\\
&+M^2(1-y^2)[(1-x)^2(1-y^2)+4\nu^2]\\
&\left.\times D_0(m^2,M^2,m^2,0,K_-^2,K_+^2,m^2,0,0,m^2)\right\},
\end{aligned} \tag{57}$$

$$\begin{aligned}
-16i\pi^2 T(x,y) &= \frac{2\nu}{M(1-x)(1-y)}\\
&\times[3B_0(0,m^2,m^2)-2\chi+5]\\
&+\frac{2\nu[B_0(K_-^2,0,m^2)-B_0(0,m^2,m^2)-1]}{M[2(1-x)(1-y)+\nu^2]}\\
&-\frac{\nu M}{2[x(1-y^2)-\nu^2]}\\
&\times\left[2(1-y)[2x+(1-x)y^2-2\nu^2]\right.
\end{aligned}$$

$$\times C_0(m^2, 0, K_-^2, 0, m^2, m^2)$$
$$- \frac{1}{(1-x)(1-y)}$$
$$\times \{2(1-y)[-2x(1-y) + (1-x^2)y^2 + (1-x)^2y^3]$$
$$+ 4v^2[1-2y(1-y)]\}C_0(m^2, M^2, K_-^2, m^2, 0, 0)$$
$$- \frac{M^2}{2}\{(1-y^2)[2x + (1-x)^2y^2] - 2v^2(1-2y^2)\}$$
$$\times D_0(m^2, M^2, m^2, 0, K_-^2, K_+^2, m^2, 0, 0, m^2)\Big]$$
$$+ (y \to -y). \tag{58}$$

In these formulas we have denoted $K_- \equiv k + p$ and $K_+ \equiv k + q$, i.e.

$$K_\pm^2 = \frac{M^2}{2}(1-x)(1 \pm y) + m^2. \tag{59}$$

The real parts of all scalar one-loop integrals used in the previous formulas can be found in [14]. We will list the scalar functions here together with the correct imaginary part:

$$B_0(0, m^2, m^2) = \frac{1}{\varepsilon} - \gamma_E + \log 4\pi + \log\left(\frac{\mu^2}{m^2}\right), \tag{60}$$

$$B_0(K_\pm^2, 0, m^2) = B_0(0, m^2, m^2)$$
$$+ 2 - \left(1 - \frac{m^2}{K_\pm^2}\right)\left[\log\left(\frac{K_\pm^2}{m^2} - 1\right) - i\pi\right], \tag{61}$$

$$C_0(m^2, 0, K_\pm^2, 0, m^2, m^2)$$
$$= \frac{1}{K_\pm^2 - m^2}\left[\frac{\pi^2}{6} - \mathrm{Li}_2\left(\frac{K_\pm^2}{m^2} + i\epsilon\right)\right]$$
$$= \frac{(-1)}{K_\pm^2 - m^2}\left[\frac{\pi^2}{6} - \mathrm{Li}_2\frac{m^2}{K_\pm^2}\right.$$
$$\left. - \log\frac{K_\pm^2}{m^2}\left(\frac{1}{2}\log\frac{K_\pm^2}{m^2} - i\pi\right)\right], \tag{62}$$

$$C_0(m^2, M^2, K_\pm^2, m^2, 0, 0) = \frac{1}{\sqrt{\lambda}}$$
$$\times \left\{2\mathrm{Li}_2(1-a_1) - \mathrm{Li}_2\left(1 - \frac{a_1}{a_2}\right) - \mathrm{Li}_2(1-a_1a_2)\right.$$
$$+ \log(a_2)\left[\log\left(\frac{K_\pm^2 - m^2}{M^2}\right) - \frac{1}{2}\log(a_2)\right]$$
$$\left. - \log(a_1)\left[\log\left(\frac{K_\pm^2 - m^2}{m^2}\right) - i\pi\right]\right\}, \tag{63}$$

where $\lambda = \lambda(m^2, M^2, K_\pm^2) = c^2 - 4m^2M^2$, $c = m^2 + M^2 - K_\pm^2$,

$$a_1 = \frac{c - 2M^2 + \sqrt{\lambda}}{c - 2M^2 - \sqrt{\lambda}}, \quad a_2 = \frac{c(c - \sqrt{\lambda})}{2m^2M^2} - 1. \tag{64}$$

Finally, the four-point function presented in the above formula is given by

$$D_0(m^2, M^2, m^2, 0, K_-^2, K_+^2, m^2, 0, 0, m^2)$$
$$= \frac{2}{M^2m^2}\frac{y}{(y^2-1)}\left\{\left(\log[2(a-1)] - i\pi\right)\log y\right.$$
$$\left. + \mathrm{Li}_2(1-y) - \mathrm{Li}_2(1-y^{-1})\right\}, \tag{65}$$

where $y = a + \sqrt{a^2 - 1}$ and

$$a = 1 + \frac{(K_-^2 - m^2)(K_+^2 - m^2)}{2M^2m^2} = 1 + \frac{1}{2v^2}(1-x)^2(1-y^2). \tag{66}$$

The soft photon approximation ($x \to 1$) needed in the main text is provided by the P form factor with the explicit result

$$P_{\mathrm{soft}}(x, y) = \frac{i}{(4\pi)^2}\frac{16v}{M^3(1-x)^2(1-y^2)}$$
$$\times [2\chi - 5 - 3B_0(0, m^2, m^2)$$
$$+ M^2C_0(m^2, M^2, m^2, m^2, 0, 0)], \tag{67}$$

while

$$A_{\mathrm{soft}}(x, y) = 0, \qquad T_{\mathrm{soft}}(x, y) = 0. \tag{68}$$

The last term in (67) is given by (cf. 8)

$$M^2C_0(m^2, M^2, m^2, m^2, 0, 0)$$
$$= \frac{1}{\sqrt{1-v^2}}\left[\mathrm{Li}_2(z) - \mathrm{Li}_2\left(\frac{1}{z}\right) + i\pi\log(-z)\right]. \tag{69}$$

References

1. A.E. Dorokhov, M.A. Ivanov, Rare decay $\pi^0 \to e^+e^-$: theory confronts KTeV data. Phys. Rev. D **75**, 114007 (2007). arXiv:0704.3498
2. A. Dorokhov, Rare decay $\pi^0 \to e^+e^-$ as a test of standard model. Phys. Part. Nucl. Lett. **7**, 229–234 (2010). arXiv:0905.4577
3. P. Vasko, J. Novotny, Two-loop QED radiative corrections to the decay $\pi^0 \to e^+e^-$: the virtual corrections and soft-photon bremsstrahlung. JHEP **1110**, 122 (2011). arXiv:1106.5956
4. S. Drell, Direct decay $\pi^0 \to e^+ + e^-$. Il Nuovo Cimento Ser. **10**(11), 693–697 (1959). doi:10.1007/BF02732327

5. E. Abouzaid et al., KTeV Collaboration, Measurement of the rare decay $\pi^0 \to e^+e^-$. Phys. Rev. D **75**, 012004 (2007). arXiv:hep-ex/0610072
6. J. Beringer et al., PDG, Review of particle physics. Phys. Rev. D **86**, 010001 (2012). doi:10.1103/PhysRevD.86.010001
7. L. Bergström, Radiative corrections to pseudoscalar meson decays. Z. Phys. C **20**, 135–140 (1983). doi:10.1007/BF01573215
8. H. Behrend et al., CELLO Collaboration, A measurement of the π^0, η and η' electromagnetic form factors. Z. Phys. C **49**, 401–410 (1991). doi:10.1007/BF01549692
9. J. Gronberg, et al., CLEO Collaboration, Measurements of the meson–photon transition form factors of light pseudoscalar mesons at large momentum transfer, Phys. Rev. D **57**, 33–54 (1998). arXiv:hep-ex/9707031
10. A. Dorokhov, E. Kuraev, Y. Bystritskiy, M. Secansky, QED radiative corrections to the decay $\pi^0 \to e^+e^-$, Eur. Phys. J. C **55**, 193–198 (2008). arXiv:0801.2028
11. Y. Kahn, M. Schmitt, T.M. Tait, Enhanced rare pion decays from a model of MeV dark matter. Phys. Rev. D **78**, 115002 (2008). arXiv:0712.0007
12. M. Knecht, A. Nyffeler, Resonance estimates of $\mathcal{O}(p^6)$ low-energy constants and QCD short distance constraints. Eur. Phys. J. C **21**, 659–678 (2001). arXiv:hep-ph/0106034
13. M. Knecht, S. Peris, M. Perrottet, E. de Rafael, Decay of pseudoscalars into lepton pairs and large-N_C QCD. Phys. Rev. Lett. **83**, 5230–5233 (1999). arXiv:hep-ph/9908283
14. K. Kampf, M. Knecht, J. Novotny, The Dalitz decay $\pi^0 \to e^+e^-\gamma$ revisited. Eur. Phys. J. C **46**, 191–217 (2006). arXiv:hep-ph/0510021
15. J. Wess, B. Zumino, Consequences of anomalous Ward identities. Phys. Lett. B **37**, 95 (1971). doi:10.1016/0370-2693(71)90582-X
16. E. Witten, Global aspects of current algebra. Nucl. Phys. B **223**, 422–432 (1983). doi:10.1016/0550-3213(83)90063-9
17. P. Frampton, Conditions for renormalizability of quantum flavor dynamics. Phys. Rev. D **20**, 3372 (1979). doi:10.1103/PhysRevD.20.3372
18. G. Passarino, M. Veltman, One-loop corrections for e^+e^- annihilation into $\mu^+\mu^-$ in the Weinberg model. Nucl. Phys. B **160**, 151–207 (1979). doi:10.1016/0550-3213(79)90234-7
19. S. Weinberg, Phenomenological Lagrangians. Physica A **96**, 327 (1979). doi:10.1016/0378-4371(79)90223-1
20. J. Gasser, H. Leutwyler, Chiral perturbation theory to one loop. Ann. Phys. **158**, 142 (1984). doi:10.1016/0003-4916(84)90242-2
21. J. Gasser, H. Leutwyler, Chiral perturbation theory: expansions in the mass of the strange quark. Nucl. Phys. B **250**, 465 (1985). doi:10.1016/0550-3213(85)90492-4
22. J. Bijnens, L. Girlanda, P. Talavera, The anomalous chiral Lagrangian of order p^6. Eur. Phys. J. C **23**, 539–544 (2002). arXiv:hep-ph/0110400
23. B. Ananthanarayan, B. Moussallam, Electromagnetic corrections in the anomaly sector. JHEP **0205**, 052 (2002). arXiv:hep-ph/0205232
24. K. Kampf, J. Novotny, Effective vertex for $\pi^0\gamma\gamma$. Acta Phys. Slov. **52**, 265 (2002). arXiv:hep-ph/0210074
25. K. Kampf, B. Moussallam, Chiral expansions of the π^0 lifetime. Phys. Rev. D **79**, 076005 (2009). arXiv:0901.4688
26. J. Bijnens, K. Kampf, S. Lanz, Leading logarithms in the anomalous sector of two-flavour QCD, Nucl. Phys. B **860**, 245–266 (2012). arXiv:1201.2608
27. M. Ramsey-Musolf, M.B. Wise, Hadronic light by light contribution to muon g-2 in chiral perturbation theory. Phys. Rev. Lett. **89**, 041601 (2002). arXiv:hep-ph/0201297
28. J. P. Miller, E. D. Rafael, B. L. Roberts, D. Stckinger, Muon (g-2): experiment and theory. Ann. Rev. Nucl. Part. Sci. **62**, 237–264 (2012). doi:10.1146/annurev-nucl-031312-120340
29. M.J. Savage, M.E. Luke, M.B. Wise, The rare decays $\pi^0 \to e^+e^-$, $\eta \to e^+e^-$ and $\eta \to \mu^+\mu^-$ in chiral perturbation theory. Phys. Lett. B **291**, 481–483 (1992). arXiv:hep-ph/9207233